

# Influence of Dynamic Disorder and Charge-Lattice Interactions on Optoelectronic Properties of Halide Perovskites

Kyle T. Munson<sup>1</sup> and John B. Asbury<sup>1,2\*</sup>

1) Materials Research Institute, The Pennsylvania State University USA.

2) Department of Chemistry, The Pennsylvania State University USA.

\*Corresponding Author: [jasbury@psu.edu](mailto:jasbury@psu.edu)

## Abstract

The origins of many unique properties of halide perovskite semiconductors can be traced to charge-lattice interactions that lead to large polaron formation combined with their unusual electronic structure of defects. However, the ability to understand and control the interplay of these electronic states with dynamic disorder arising from structural fluctuations of the metal halide framework is needed to guide continued development of new variants of these materials. In this perspective, we examine the influence that dynamic disorder has on charge-lattice interactions in halide perovskite materials that lead to charge localization and large polaron formation. Furthermore, we describe how the interplay of material composition, structural dynamics and large polaron formation influences radiative and non-radiative band-edge recombination. Insights about how to control this interplay may inform development of related metal halide semiconductors including 2D Ruddlesden-Popper, double perovskites and nanocrystalline systems with tailored radiative and charge transport properties while avoiding toxic elements.

## Introduction

The extraordinary performance of halide perovskite-based photovoltaics is mainly due to the low nonradiative recombination rates,<sup>1</sup> micrometer carrier diffusion lengths,<sup>2</sup> and microsecond carrier lifetimes<sup>3-4</sup> exhibited in this material class. These properties enable halide perovskite photovoltaic devices to exhibit high open-circuit voltages despite being processed from solution.<sup>5</sup> Halide perovskites also possess other favorable optoelectronic properties, such as small exciton binding energies<sup>6</sup> and high absorption coefficients,<sup>7</sup> making them ideal materials for a wide variety of optoelectronic applications beyond photovoltaics such as lasers<sup>8-9</sup> and LEDs.<sup>10</sup>

There is growing consensus in the literature that charge-lattice interactions cause charge carriers to self-trap into large polaronic states and that these states figure prominently in the remarkable optoelectronic properties of halide perovskite materials.<sup>11-20</sup> For example, contemporary work using far-IR, terahertz, or Raman spectroscopy to examine polaron frequencies and estimates of dielectric properties and carrier effective masses demonstrates that this coupling is well described by Fröhlich-type interactions of charges with polar phonon modes in methylammonium lead halide perovskites.<sup>21-24</sup> These polaronic states are considered to be 'large' in halide perovskites because the polarization cloud created by distortions of the perovskite lattice around charge carriers span several unit cells.<sup>20</sup>

The formation of large polarons is thought to be the origin of the slow second order recombination rates and moderate charge carrier mobilities exhibited in three-dimensional perovskites.<sup>25</sup> Consistent with this hypothesis, recent theoretical work has suggested that the lattice fluctuations that lead to polaron formation may generate repulsive interactions between oppositely charged carriers.<sup>11</sup> Lattice fluctuations may also affect the cooling rates of above-band-gap "hot" carriers following optical excitation.<sup>26-27</sup> In particular, the formation of large polarons may suppress the carrier scattering events that lead to carrier cooling in halide perovskites.<sup>28</sup>

The above reports highlight the need to understand the interplay between dynamic disorder due to fluctuations of the perovskite lattice<sup>12, 21</sup> and the charge-lattice interactions that lead to polaron formation<sup>21-24</sup> Furthermore, the exact nature of the charge-lattice interactions, how they are modulated by the underlying structure and composition, and how these in turn affect the optoelectronic properties of metal halide perovskites has not been fully elucidated. Such knowledge will be critical for understanding how the reduced dimensionality and modified crystal structures of metal halide semiconductors such as 2D Ruddlesden Popper<sup>29-31</sup> and double perovskite materials<sup>32-34</sup> influence their light emitting and optoelectronic properties.

In this Perspective, we describe recent experimental studies that used temperature-dependent, mid-infrared transient absorption (mid-IR TA) spectroscopy and time-resolved photoluminescence (TRPL) spectroscopy to examine the effect of large polaron formation on band-edge recombination in halide perovskites at carrier densities closely matched to those of operating photovoltaic devices to minimize higher order recombination artifacts. We then highlight recent measurements of the structural fluctuations that are correlated with large polaron formation using mid-IR TA spectroscopy to probe the vibrational dynamics of the halide perovskite lattice. Furthermore, we examine the influence that various A-site cations have on the dynamics of large polaron formation, their delocalization lengths, binding energies, and influence on charge recombination using a series of lead bromide perovskite films. Finally, we discuss how the charge-lattice interactions that lead to polaron formation may be modified by ion substitution and suggest future studies using mid-IR TA spectroscopy that can be used to build structure-function correlations to predict how the compositions of new metal halide semiconductors influence their optoelectronic and light emitting properties.<sup>29-34</sup>

## Results and Discussion

The three-dimensional halide perovskites utilized in state-of-the-art photovoltaic devices share a common  $ABX_3$  structure where A is a monovalent cation, B is a divalent metal ion, and X is a halide anion (Figure 1A).<sup>35-36</sup> The A-site ion used to form halide perovskites are typically either small organic molecules, such as methylammonium (MA) and formamidinium (FA), or inorganic ions such as cesium (Cs). Lead (Pb) and tin (Sn) are commonly used as the B-site metal ion. Iodide ( $I^-$ ) and bromide ( $Br^-$ ) anions typically occupy the X site of the perovskite structure. However, chloride ( $Cl^-$ ) anions also have been used. Interestingly, the composition of state-of-the-art perovskite devices commonly includes several different A-site cations, B site metal ions, and X site halide ions such as  $FA_{0.79}MA_{0.16}Cs_{0.05}Pb_{0.85}Sn_{0.15}I_{2.5}Br_{0.5}$ .<sup>5</sup>

In stark contrast to other inorganic semiconductors such as Si and GaAs, the halide perovskite lattice is mechanically soft and dynamically disordered.<sup>12</sup> A variety of experimental methods have been used to examine the anharmonic nature of the perovskite lattice.<sup>14, 37-38</sup> For

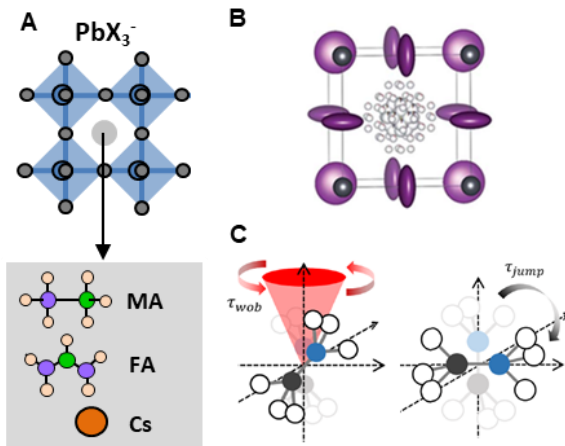


**Figure 1.** **A.** Representation of the perovskite unit cell depicting the inorganic  $AX_3$  framework and the structure of common A site cations used in state-of-the-art devices. Reprinted with permission from Ref 28. Copyright 2016 American Chemical Society. **B.** Refined structure of a  $MAPbI_3$  single crystal obtained from neutron diffraction measurements. The structure highlights the disordered nature of the perovskite's MA cations and the large displacement (ellipsoids) of the material's halide ions. Reprinted with permission from Ref 40. Copyright 2015 Royal Society of Chemistry. **C.** Cartoon representation of the rotational motion of MA cations in halide perovskites. Reprinted with permission from Ref 42. Copyright 2018 American Chemical Society.

example, Raman spectroscopy and molecular dynamics simulations have shown that the low-frequency vibrational modes of the perovskite lattice's  $\text{BX}_3$  framework undergo large amplitude displacements at room temperature.<sup>39</sup> Likewise, neutron diffraction measurements also have been used to investigate the structural dynamics of the perovskite lattice.<sup>40</sup> **Figure 1B** shows the refined structure of a  $\text{MAPbI}_3$  perovskite single crystal obtained from neutron diffraction measurements. The structure highlights the atomic displacements of the iodine atoms that arise from the anharmonic nature of the perovskite lattice at room temperature. These displacements are represented as ellipsoids in the figure. The structure also highlights the disordered nature of the MA cations, which appear as a "sphere" in the center of the  $\text{BX}_3$  framework.

Organic cations in hybrid organic-inorganic perovskites, such as  $\text{MAPbI}_3$ , interact with the material's inorganic framework mainly via ion-ion, ion-dipole, and hydrogen bonding interactions.<sup>41</sup> However, in the high-temperature tetragonal and cubic phases of the material, these interactions are not strong enough to immobilize the organic ions.<sup>42</sup> As a result, organic cations can rotate rapidly within the perovskite lattice's  $\text{BX}_3$  framework. Numerous experimental reports have examined the rotational dynamics of organic cations in halide perovskites. For example, polarization-resolved two-dimensional infrared (2DIR) spectroscopy was used to investigate the rotational motion of MA ions in halide perovskites.<sup>43-44</sup> From these measurements, the authors determined that MA cations in  $\text{MAPbI}_3$  perovskite films undergo two distinct wobbling-in-cone ( $\sim 0.3$  ps) and rotational motions ( $\sim 3$  ps), respectively (**Figure 1C**). Similar dynamics also were obtained from polarization resolved 2DIR measurements of FA ions in  $\text{FAPbI}_3$  thin films.<sup>45</sup> For more information about the rotational dynamics of organic cations, we direct the reader to a recent perspective from Bakulin and coworkers.<sup>42</sup>

The disordered nature of both the inorganic  $\text{BX}_3$  framework and A-site cations has led several investigators to propose that fluctuations of the perovskite lattice underpin the remarkable optoelectronic properties exhibited in this class of material.<sup>46-48</sup> Evidence for charge-lattice

interactions arising from electron-phonon coupling in halide perovskites has been obtained from temperature-dependent PL,<sup>49</sup> charge carrier mobility,<sup>18, 47</sup> two-dimensional electronic spectroscopy,<sup>50</sup> and THz measurements.<sup>23, 51</sup> Such experiments led investigators to propose that fluctuations of the perovskite lattice cause charge carriers to self-trap into large polaronic states within the material.<sup>12, 20, 25</sup> These studies also revealed that the charge-lattice coupling in metal halide perovskites is relatively weak, consistent with Frohlich-type interactions of charge carriers with polar LO phonons.<sup>21-24</sup> The formation of large polarons prolongs the recombination lifetimes of charge carriers<sup>12, 20</sup> and may also shield charge carriers from defects within the material.<sup>52</sup> It is likely that these properties facilitate the ability to deposit high-performance halide perovskite materials using a variety of solution-processed deposition methods.<sup>53</sup>

The connection between the structural and electronic properties of halide perovskites has encouraged studies that investigate the dynamics of charge carriers in these materials following photoexcitation.<sup>35, 54</sup> However, it has been challenging to draw direct correlations between structural fluctuations and polaron dynamics using traditional spectroscopic techniques, such as TRPL alone. In part, this is due to TRPL measurements being affected only indirectly by non-radiative recombination pathways among the band-edge states of the material and because numerous processes can contribute to the observed spectra and kinetics.<sup>55</sup>

Recently, advances in mid-IR TA spectroscopy have enabled the technique to be used to directly probe the spectroscopic signatures of large polarons in halide perovskites at low photogenerated charge carrier densities ( $3 \cdot 10^{16} \text{ cm}^{-3}$ ) following optical excitation at 532 nm and 500 nJ/cm<sup>2</sup>.<sup>12</sup> These excitation conditions produce transient carrier densities that closely resemble carrier densities that occur under steady-state solar illumination,<sup>56-57</sup> allowing the dynamics of large polarons to be measured under conditions relevant to functioning optoelectronic devices. **Figure 2A** shows the large polaron spectra obtained from mid-IR TA spectroscopy measurements of a polycrystalline MAPbI<sub>3</sub> film following a 30 ns time delay after bandgap excitation.<sup>12</sup> Such

polycrystalline  $\text{MAPbI}_3$  films will be called simply  $\text{MAPbI}_3$  films here and in the following. The inset of **Figure 2A** shows the transitions that appear in the spectrum. The absorption spectra of large polarons are characterized by a sharp absorption onset at a transition energy three times the large polaron self-trapping energy and a Drude-like free carrier absorption tail at higher transition energies.<sup>58</sup> The origin of this behavior can be traced to a combination of short and long-range charge-lattice interactions that define the kinetic and potential energies of charge carriers interacting with their self-generated polarization clouds in the inorganic sublattice. The spectrum appearing in **Figure 2A** also shows narrow vibrational features of the MA cations within the  $\text{MAPbI}_3$  film. These vibrational features serve as direct probes of the structural dynamics of the perovskite lattice in the presence of charge carriers. Consequently, analysis of these vibrational features enabled the investigators to obtain mechanistic information about the structural origin of polaron formation in halide perovskites optoelectronic materials. The measurements of the excited-state vibrational dynamics of the perovskite lattice are discussed below.

The ability to measure the dynamics of large polarons at low excitation densities enabled their dynamics to be directly compared to TRPL measurements under identical conditions (**Figure 2B**).<sup>12</sup> **Figure 2C** displays normalized recombination kinetics of large polarons (from their mid-IR absorptions) compared with the normalized PL decays of a  $\text{MAPbI}_3$  film measured under identical conditions (532 nm, 500  $\text{nJ}/\text{cm}^2$  excitation density) at 190 and 290 K. We note that analysis of the shapes of the large polaron absorption spectra appearing in **Figure 2A** as a function of temperature allowed investigators to determine that the delocalization length of large polarons decreased from  $\sim 11$  nm at 190 K to  $\sim 9$  nm at 290 K, indicating that charge carriers were more spatially localized at higher temperatures.<sup>20</sup> Thus, comparing the large polaron and TRPL decay kinetics allowed the effects of carrier localization on band-edge recombination to be determined.

At lower temperature (190 K), where charge carriers are more delocalized, the TRPL dynamics exhibited band-edge emission in quantitative agreement with the dynamics of charge carriers probed using mid-IR TA spectroscopy (**Figure 2C**, left). However, at room temperature (290 K), the lifetime of charge carriers probed in the mid-IR increased 20-fold relative to the lower temperature measurement and deviated from the radiative recombination kinetics measured using TRPL under the same conditions (**Figure 2C**, right). These results are also consistent with temperature-dependent measurements of bimolecular recombination coefficients,<sup>20</sup> which showed that charge carrier localization also decreases bimolecular recombination rates within the material.

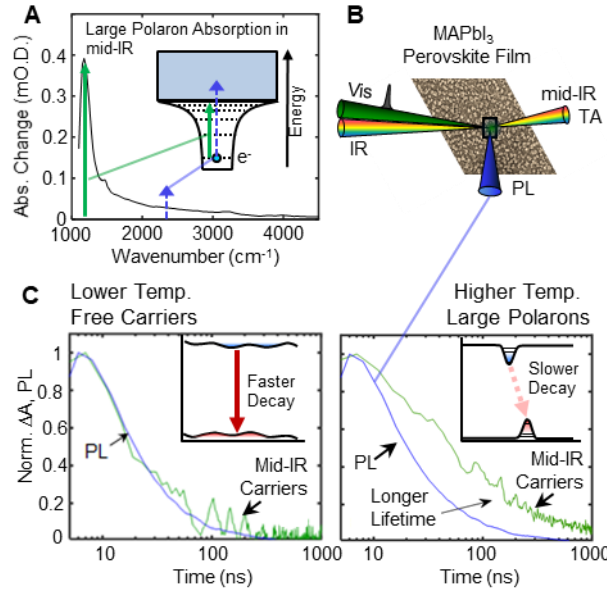


**Figure 2.** **A.** Mid-IR TA spectrum of large polarons in a halide perovskite film measured at a 30 ns time delay following band-gap excitation. The inset shows the transitions that appear in the spectrum. The inset depicts the transitions that appear in the spectrum. **B.** Schematic showing TRPL and TRIR measurements performed under identical low excitation density conditions. **C.** TRPL decay versus mid-IR TA recombination kinetics measured at 290 K (right) and 190 K (left) plotted on a logarithmic time axis. The mid-IR TA and TRPL decay kinetics match within experimental precision at lower temperature but deviate at higher temperature because of carrier localization caused by charge-lattice interactions that are enhanced by dynamic disorder at elevated temperatures. Reprinted with permission from Ref 12. Copyright 2018 Elsevier.

The above comparison reveals that the localization of charge carriers into large polaronic states at elevated temperatures slows charge carrier recombination within the material. However, the formation of large polarons also quenches photoluminescence (**Figure 2C**, Ref 12). Thus, while polaron formation may be advantageous for photovoltaic devices due to prolonged charge carrier lifetimes, it may hinder the efficiencies of perovskite-based LEDs.<sup>59</sup> For example, the efficiencies of light emitting diodes fabricated using two-dimensional (2D) lead-halide perovskites are typically low<sup>59</sup> and, in some cases, can only be measured at cryogenic temperatures.<sup>60-61</sup> These poor efficiencies may be due to enhanced electron-phonon interactions and polaron formation within the material, which has been reported previously by Silva and coworkers.<sup>16</sup> However, certain intrinsic distortions in low dimensional halide perovskites can lead to polaronic excitons with efficient broadband emission.<sup>29-30</sup> These observations underscore the need to understand the interplay of such polaronic effects on excited electronic states to predict and control the electronic properties of halide perovskites.

Because the formation of large polarons in halide perovskites slows charge recombination and quenches photoluminescence, modifying the charge-lattice interactions that lead to polaron formation may allow investigators to tune the optoelectronic properties of halide perovskites for specific applications, such as light-emitting diodes and lasers. To this end, several investigators have examined the excited-state phonon dynamics in lead-halide perovskites that lead to polaron formation.<sup>14</sup> For example, time-domain Raman (TDR) measurements of a  $\text{MAPbBr}_3$  film collected after excitation of the material's bandgap using ultrashort laser pulses suggested that the presence of photogenerated charge carriers shifts the equilibrium positions and vibrational energies of the perovskite lattice.<sup>24</sup> Likewise, time domain optical Kerr effect (OKE) spectroscopy has previously been used to probe the relaxation of the perovskite lattice's Pb-X modes following optical excitation.<sup>13</sup>

As stated above, mid-IR TA spectroscopy is also capable of measuring the excited state vibrational dynamics that are correlated with polaron formation in halide perovskites. **Figure 3A** displays baseline corrected mid-IR TA spectra of a  $\text{MAPbI}_3$  film collected in the MA cation's symmetric N-H bend region measured at 310 K and 190 K.<sup>20</sup> The vibrational features depicted in the mid-IR TA spectra arise from perturbations of the symmetric N-H bend mode caused by the

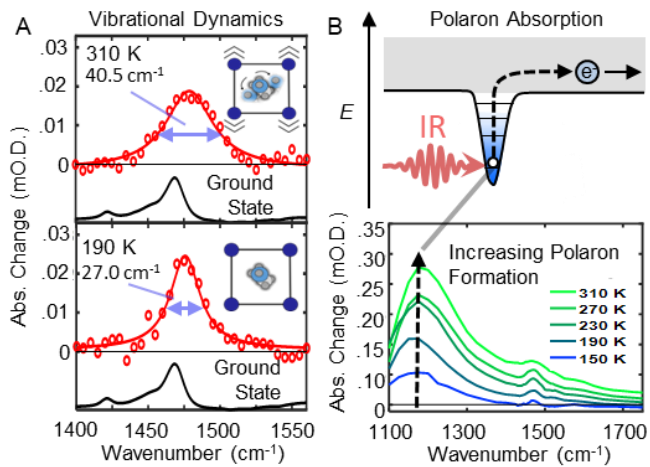


**Figure 3. A.** Baseline corrected mid-IR TA spectra of a  $\text{MAPbI}_3$  film in its excited electronic state collected at 190 and 310 K following bandgap excitation at 532 nm. The spectra highlight the N-H bend region of the film. The smooth curves through the data represent the Lorentzian functions used to quantify the full width at half maximum of the vibrational features. Corresponding FTIR spectra are shown below the mid-IR TA spectra for comparison. Reprinted with permission from Ref 20. Copyright 2019 American Chemical Society. **B.** Polaron absorption spectra of a  $\text{MAPbI}_3$  film measured at different temperatures following bandgap excitation. The density of absorbed photons was identical for all temperatures, indicating that the increase in amplitude of the large polaron spectra at elevated temperatures is due to enhanced polaron formation. Reprinted with permission from Ref 12. Copyright 2018 Elsevier.

presence of photogenerated charge carriers in the excited electronic state of the halide perovskite film. The corresponding ground-state FTIR spectra of the film at each temperature appear in the lower panels of **Figure 3A**. Similar perturbations were observed of N-H and C-H stretch vibrational modes in a  $\text{MAPbI}_3$  film using recent time-resolved<sup>55</sup> and steady-state mid-IR measurements.<sup>62</sup>

Unlike the FTIR spectra, both the center frequency and line width of the N-H bend mode change with temperature in the excited electronic state. The N-H bend vibrations of the

excited electronic state were fit with Lorentzian functions to quantify the changes in their line widths. The best fit functions are overlaid on the vibrational spectra shown in **Figure 3A**. The increase in the linewidth of the vibrational mode at 310 K indicates faster vibrational dephasing of the N-H bend vibrational mode in the excited electronic state at elevated temperatures. These faster vibrational dephasing dynamics originate from structural distortions of the perovskite lattice that change the hydrogen bonding and ion-dipole interactions between MA cations and the material's  $\text{PbI}_3^-$  inorganic framework.<sup>20</sup>

The faster vibrational dephasing dynamics observed in **Figure 3A** at elevated temperatures were correlated with the self-trapping of charge carriers into large polaronic states. **Figure 3B** shows temperature-dependent polaron absorption spectra collected under the same experimental conditions as the vibrational dynamics.<sup>12</sup> The temperature-dependent study reveals that the intensity of the mid-IR polaron absorption feature increases as the temperature was raised, indicating that large polaron formation is enhanced at elevated temperatures when the perovskite lattice undergoes larger amplitude fluctuations. This increase of large polaron formation was associated with a corresponding decrease of the radiative quantum yield at elevated temperatures from TRPL measurements.<sup>12</sup> The TRPL and mid-IR TA measurements were conducted with the same excitation intensities at all temperatures, allowing quantitative comparison of the changes of radiative efficiencies with the variation of the densities of large polarons. Taken together, these results indicate that temperature dependent anharmonic fluctuations of the perovskite lattice enhance the charge-lattice interactions that underpin polaron formation and recombination mechanisms in the excited state of this class of material.

Because polaron formation depends on the structural dynamics of the halide perovskite lattice, several reports have investigated the influence that the material's A-site cations and inorganic  $\text{BX}_3$  framework have on polaron formation and recombination mechanisms. Both computational and experimental reports have suggested that the motion of dipolar organic cations

affects polaron formation, transport, and recombination in halide perovskites.<sup>25, 63-68</sup> For example, the orientational motion of FA cations in FAPbI<sub>3</sub> films was suggested to influence the electronic properties of halide perovskites on the basis of temperature-dependent photoluminescence measurements.<sup>63</sup> However, temperature-dependent Raman spectroscopy measurements revealed that the polar fluctuations which underpin polaron formation in halide perovskites do not depend on the dipole moment of the material's A-site cation.<sup>39</sup>

To address whether the dipolar motion of A-site cations influences charge carrier dynamics in halide perovskites, investigators used mid-IR TA spectroscopy to examine polaron formation and charge recombination in halide perovskites with different types of A-site cations.<sup>36</sup>

**Figure 4A** shows the large polaron absorption spectra of MAPbBr<sub>3</sub>, FAPbBr<sub>3</sub>, and CsPbBr<sub>3</sub> perovskite films measured under identical excitation conditions. The similarity between the mid-IR TA spectra, whose shape depends on the delocalization length and binding energies of large polarons,<sup>20, 36</sup> indicated that the dipolar disorder (or alignment) of organic cations within the perovskite lattice does not influence the extent of carrier localization or large polaron binding energies.

The influence of dipolar organic cations on the optoelectronic properties of halide perovskites was further investigated by examining the decay kinetics of the large polaron absorption spectra shown in **Figure 4A**. **Figures 4B** represents polaron decay kinetics of MAPbBr<sub>3</sub>, FAPbBr<sub>3</sub>, and CsPbBr<sub>3</sub> films obtained by integrating the frequency range between 1000-1800 cm<sup>-1</sup> following 532 nm pulsed excitation. The comparison shows little variation in the lifetime of large polarons photogenerated within each of the perovskite films. Additional analysis of the decay kinetics using a method previously developed to examine polaron recombination dynamics in MAPbI<sub>3</sub> films revealed that the bimolecular recombination coefficients for the perovskite films examined in **Figure 4** were indistinguishable within experimental precision. This finding is consistent with prior time-resolved terahertz spectroscopy measurements of CsPbI<sub>3</sub>.

films that showed similar charge transport and recombination kinetics compared to their hybrid organic-inorganic  $\text{MAPbI}_3$  analogs.<sup>69</sup> Taken together, these results indicate that the dipolar field created by organic cations does not affect recombination rates in halide perovskites. Instead, the charge-lattice interactions leading to polaron formation, slower recombination rates, and quenched photoluminescence arise from distortions of the material's inorganic sublattice.

The ability to probe the mid-infrared optical absorption spectra of large polarons in halide perovskites also allowed investigators to determine if dipolar organic cations influence carrier localization on ultrafast timescales. As mentioned previously, some investigators have suggested that polaron formation in halide perovskite affects carrier cooling rates within the material.<sup>27-28</sup>

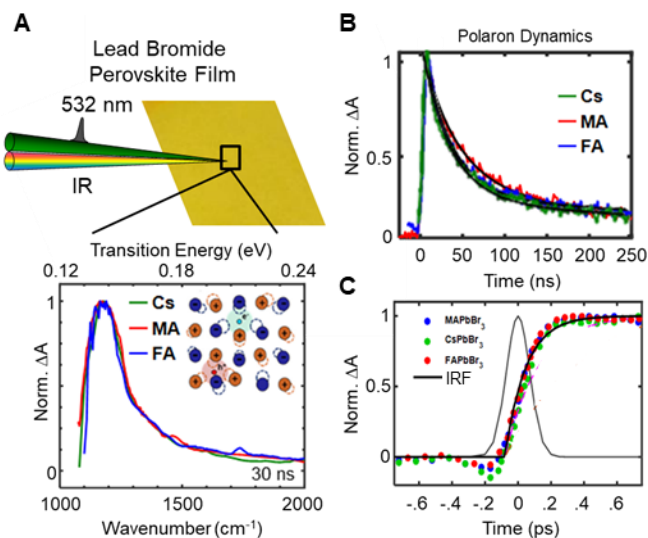


**Figure 4.** **A.** (top) Schematic diagram of the mid-IR TA optical geometry. (bottom) Mid-IR TA spectra of  $\text{MAPbBr}_3$ ,  $\text{FAPbBr}_3$ , and  $\text{CsPbBr}_3$  perovskite films. **B.** Polaron decay kinetics of  $\text{MAPbBr}_3$ ,  $\text{FAPbBr}_3$ , and  $\text{CsPbBr}_3$  perovskite films following bandgap excitation at 532 nm. The comparisons demonstrate that the dipolar motion of organic cations does not affect polaron spectra or recombination rates within the material. **C.** Polaron formation kinetics measured in the series of lead bromide perovskite films following optical excitation at 532 nm. The polaron formation rates are identical despite the different dipole moments of the A site cations, indicating that organic cation rotations do not contribute significantly to polaron formation in halide perovskites. Reprinted with permission from Ref 36. Copyright 2020 American Chemical Society.

Thus, understanding how to control polaron formation rates in halide perovskites may lead to the development of design rules for how to utilize hot carriers in perovskite-based optoelectronics.

**Figure 4C** displays the ultrafast mid-IR TA kinetics of the large polaron absorption signal presented in **Figure 4A** following pulsed excitation at 532 nm.<sup>36</sup> The formation rate of large polarons in each film was estimated by monitoring the growth of the large polaron absorption signal. For all of the ultrafast mid-IR TA kinetics displayed in **Figure 4C**, the rise time of the transient absorption signal was limited by the instrument response of the ultrafast measurement (grey line, **Figure 4C**), indicating that polarons form rapidly in halide perovskites in less than 150 fs following optical excitation. Importantly, the results presented in **Figure 4C** indicate that polaron formation rates do not depend on the identity of the A-site cation. Furthermore, the rise times of the polaron absorption signals are significantly faster than the diffusive motion of organic cations (~3 ps) obtained by polarization-resolved 2DIR measurements,<sup>42</sup> indicating that the dipolar motion of organic cations does not underpin polaron formation in this class of material. Rather, distortions of the inorganic sublattice underpin polaron formation on ultrafast timescales in halide perovskites. This result is consistent with low-frequency Raman spectroscopy measurements, which revealed that polar fluctuations underpinning polaron formation do not depend on the dipole moment of the A-site cation in this class of material.<sup>39</sup> Likewise, theoretical calculations have also shown that Fröhlich interactions between charge carriers and phonons occur predominately with the stretching and bending LO phonon modes of the material's  $\text{PbI}_3$  inorganic sublattice.<sup>70</sup> The above findings reveal that mixtures of A-site cations that can affect the optoelectronic properties of halide perovskites<sup>25, 63-68</sup> may do so by their influence on the structure and dynamics of the inorganic lattice rather than from the dipolar properties of the cations themselves. These observations further highlight the need to understand the interplay of such polaronic effects on excited electronic states to predict and control the electronic properties of halide perovskites.

These findings also suggest that efforts to tune the properties of halide perovskites for photovoltaic and light emitting applications should similarly focus on the structure and dynamics of the inorganic sublattice and how organic A-site cations may influence this sublattice. Recent theoretical studies have suggested that it may be possible to tune the structural dynamics of the perovskite lattice that lead to polaron formation by incorporating ions with different sizes into the material.<sup>46, 71</sup> **Figure 5A** highlights one of these studies, which suggested that the mixing of differently sized A-site cations (e.g., FA and Cs) within the perovskite lattice may slow the dynamics of the perovskite lattice by effectively “locking” the material’s inorganic framework.<sup>46</sup> Such reduced lattice fluctuations may lead to smaller charge-lattice coupling and would be expected to slow the rotational dynamics of the FA cations, consistent with the molecular dynamics (MD) simulations that examined the dynamics of FA cations in mixed-cation perovskites (**Figure 5A**). The results of these MD simulations were later confirmed experimentally in a perspective written by Gallop and coworkers who used 2DIR anisotropy to examine the dynamics of FA cations in mixed and pure cation perovskite films (**Figure 5B**).<sup>42</sup>

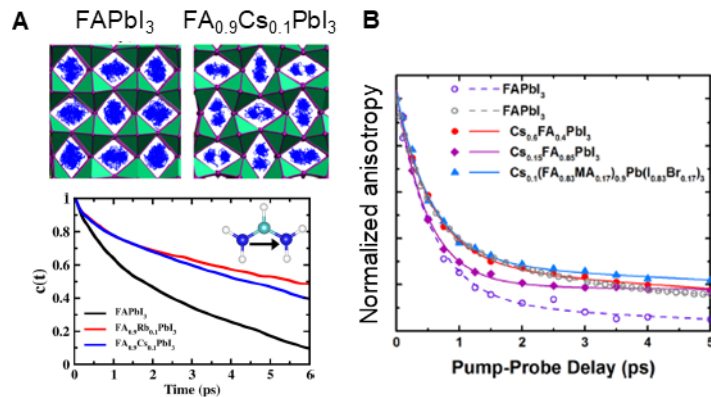


**Figure 5. A.** (top) Plot showing the positions of nitrogen atoms of FA over time in pure and mixed-phase perovskite films. (bottom) Vector autocorrelation function of FA cations in mixed and pure phase perovskite films obtained from molecular dynamics simulations showing the probability of a FA cation remaining in its initial orientation as a function of time. Reprinted with permission from Ref 46. Copyright 2017 American Chemical Society. **B.** Transient anisotropy dynamics of FA ions obtained by measuring the CN stretch mode. Reprinted with permission from ref 42. Copyright 2018 American Chemical Society.

Recalling that the composition of current state-of-the-art perovskite-based devices includes several different A-site cations, B site metal ions, and X site halide ions, the results presented in **Figure 5** suggest that device developers may be tuning the polaronic properties of halide perovskites via ion substitution to strike the optimal balance between charge transport and recombination for photovoltaic applications. For example, mixed cation systems with various MA, FA and Cs ion ratios can exhibit enhanced photoluminescence quantum yields and slower defect-mediated recombination.<sup>42, 72-74</sup> Additionally, ion substitution may also introduce static disorder that may lead to disordered charge–lattice coupling and polaron formation, as has recently been reported by Nishida and coworkers.<sup>75</sup> Such static disorder may also slow charge carrier recombination by spatially separating charge carriers in separate regions of a film.<sup>76</sup> Continued work that correlates polaron recombination rates and transport in mixed ion perovskites with device results is expected to be an active area of research in the perovskite community.

### ***Conclusions and Outlook***

In this perspective, recent mid-IR TA spectroscopy studies were highlighted that examined the charge-lattice interactions and dynamic disorder that lead to large polaron formation. The influence these interactions have on band-edge recombination and optoelectronic properties of halide perovskites were also discussed. The formation of large polarons was shown to slow bimolecular recombination within the materials. However, the energetic barriers introduced by polaron formation also quench photoluminescence quantum yields. This result suggests that the electronic properties of halide perovskites can be tuned for specific applications (e.g., photovoltaics vs. light emitting diodes) by modifying the structure and composition of the materials. Furthermore, the results presented in this perspective demonstrate that the dipolar motion of organic cations does not affect polaron formation or bimolecular recombination in halide perovskites, indicating that investigators should focus on understanding how modifications to the

structure and dynamics of the perovskite lattice's inorganic framework affect the charge-lattice interactions that underpin polaron formation.

While clarity is emerging about the influence that charge-lattice interactions have on the electronic properties of traditional halide perovskites such as  $\text{MAPbI}_3$  and related materials, the ability to predict and control these interactions in more complex metal halide semiconductors such as 2D Ruddlesden Popper layered materials, double perovskites and nanocrystalline systems remains to be developed. Future work leveraging the structural specificity of mid-IR TA spectroscopy combined with the ability to measure the energetics and dynamics of large polarons is expected to help guide ongoing efforts to understand the nature of charge-lattice interactions in these materials. For example, investigators may use mid-IR TA spectroscopy to directly probe the vibrational modes of organic cations that separate the layers in 2D Ruddlesden Popper materials<sup>29-31</sup> to investigate the structural distortions and lattice dynamics involved in charge transport versus radiative recombination. Similar approaches may be used to investigate the lattice dynamics in double perovskites with mixed +1 and +3 cations being investigated as lead-free alternatives<sup>32-34</sup> to guide exploration of the large parameter space of these materials to achieve desired material properties.

Finally, the results presented in the perspective suggest that charge carrier cooling dynamics in halide perovskites can be investigated using mid-IR TA spectroscopy.<sup>36</sup> Both theoretical and experimental studies have suggested that the unusually slow thermalization kinetics observed in halide perovskites may be due to the polaronic nature of charge carriers in this class of material. Thus, carrier cooling rates in halide perovskite films may be characterized on ultrafast time scales by directly probing the optical signatures of large polarons in the mid-IR as a function of excitation wavelength and temperature. Because polaron formation is temperature-dependent<sup>12</sup>, these measurements are expected to provide information about how polaron formation affects carrier thermalization in this class of material.

## **Author Information**

### **Corresponding Author**

J.B.A.: [jasbury@psu.edu](mailto:jasbury@psu.edu)

### **Acknowledgements**

The authors K. T. M. and J. B. A. are grateful for support of this work from the U.S. National Science Foundation under Grant Number CHE-1954301. K. T. M. is grateful for support from the National Science Foundation Graduate Research Fellowship Program under Grant No. DGE1255832. Any opinions, findings, and conclusions or recommendations expressed in this material are those of the author(s) and do not necessarily reflect the views of the National Science Foundation.

### **DECLARATION OF INTERESTS**

J.B.A. owns equity in Magnitude Instruments, which has an interest in this project. His ownership in this company has been reviewed by the Pennsylvania State University's Individual Conflict of Interest Committee and is currently being managed by the University.

## **References**

1. deQuilettes, D. W.; Frohna, K.; Emin, D.; Kirchartz, T.; Bulovic, V.; Ginger, D. S.; Stranks, S. D., Charge-Carrier Recombination in Halide Perovskites. *Chem. Rev.* **2019**, *119*, 11007-11019.
2. Stranks, S. D.; Eperon, G. E.; Grancini, G.; Menelaou, C.; Alcocer, M. J. P.; Leijtens, T.; Herz, L. M.; Petrozza, A.; Snaith, H. J., Electron-Hole Diffusion Lengths Exceeding 1 Micrometer in an Organometal Trihalide Perovskite Absorber. *Science* **2013**, *342*, 341-344.
3. deQuilettes, D. W.; Koch, S.; Burke, S.; Paranjpye, R. K.; Shropshire, A. J.; Ziffer, M. E.; Ginger, D. S., Photoluminescence Lifetimes Exceeding 8 Ms and Quantum Yields Exceeding 30% in Hybrid Perovskite Thin Films by Ligand Passivation. *ACS Energy Lett.* **2016**, *1*, 438-444.

4. Stewart, R. J.; Grieco, C.; Larsen, A. V.; Maier, J. J.; Asbury, J. B., Approaching Bulk Carrier Dynamics in Organo-Halide Perovskite Nanocrystalline Films by Surface Passivation. *J. Phys. Chem. Lett.* **2016**, *7*, 1148-1153.
5. Gratzel, M., The Rise of Highly Efficient and Stable Perovskite Solar Cells. *Acc. Chem. Res.* **2017**, *50*, 487-491.
6. Chen, X.; Lu, H.; Yang, Y.; Beard, M. C., Excitonic Effects in Methylammonium Lead Halide Perovskites. *J. Phys. Chem. Lett.* **2018**, *9*, 2595-2603.
7. De Wolf, S.; Holovsky, J.; Moon, S.-J.; Löper, P.; Niesen, B.; Ledinsky, M.; Haug, F.-J.; Yum, J.-H.; Ballif, C., Organometallic Halide Perovskites: Sharp Optical Absorption Edge and Its Relation to Photovoltaic Performance. *J. Phys. Chem. Lett.* **2014**, *5*, 1035-1039.
8. Jia, Y. F.; Kerner, R. A.; Grede, A. J.; Rand, B. P.; Giebink, N. C., Continuous-Wave Lasing in an Organic-Inorganic Lead Halide Perovskite Semiconductor. *Nat. Photon.* **2017**, *11*, 784-788.
9. Jia, Y.; Kerner, R. A.; Grede, A. J.; Brigeman, A. N.; Rand, B. P.; Giebink, N. C., Diode-Pumped Organo-Lead Halide Perovskite Lasing in a Metal-Clad Distributed Feedback Resonator. *Nano Lett.* **2016**, *16*, 4624-4629.
10. Wang, H.; Kosasih, F. U.; Yu, H.; Zheng, G.; Zhang, J.; Pozina, G.; Liu, Y.; Bao, C.; Hu, Z.; Liu, X., et al., Perovskite-Molecule Composite Thin Films for Efficient and Stable Light-Emitting Diodes. *Nat. Commun.* **2020**, *11*, 891.
11. Emin, D., Barrier to Recombination of Oppositely Charged Large Polarons. *J. Appl. Phys.* **2018**, *123*, 055105.
12. Munson, K. T.; Kennehan, E. R.; Doucette, G. S.; Asbury, J. B., Dynamic Disorder Dominates Delocalization, Transport, and Recombination in Halide Perovskites. *Chem* **2018**, *4*, 2826-2843.
13. Miyata, K.; Meggiolaro, D.; Trinh, M. T.; Joshi, P. P.; Mosconi, E.; Jones, S. C.; De Angelis, F.; Zhu, X. Y., Large Polarons in Lead Halide Perovskites. *Sci. Adv.* **2017**, *3*, e1701217.
14. Munson, K. T.; Swartzfager, J. R.; Asbury, J. B., Lattice Anharmonicity: A Double-Edged Sword for 3d Perovskite-Based Optoelectronics. *ACS Energy Lett.* **2019**, *4*, 1888-1897.
15. Tsai, H.; Asadpour, R.; Blancon, J.-C.; Stoumpos, C. C.; Durand, O.; Strzalka, J. W.; Chen, B.; Verduzco, R.; Ajayan, P. M.; Tretiak, S., et al., Light-Induced Lattice Expansion Leads to High-Efficiency Perovskite Solar Cells. *Science* **2018**, *360*, 67-70.
16. Kandada, A. R. S.; Silva, C., Exciton Polarons in Two-Dimensional Hybrid Metal-Halide Perovskites. *J. Phys. Chem. Lett.* **2020**, *11*, 3173-3184.
17. Bretschneider, S. A.; Ivanov, I.; Wang, H. I.; Miyata, K.; Zhu, X.; Bonn, M., Quantifying Polaron Formation and Charge Carrier Cooling in Lead-Iodide Perovskites. *Adv. Mater.* **2018**, *30*, 1707312.
18. Bonn, M.; Miyata, K.; Hendry, E.; Zhu, X. Y., Role of Dielectric Drag in Polaron Mobility in Lead Halide Perovskites. *ACS Energy Lett.* **2017**, *2*, 2555-2562.
19. Zhu, H.; Miyata, K.; Fu, Y.; Wang, J.; Joshi, P. P.; Niesner, D.; Williams, K. W.; Jin, S.; Zhu, X.-Y., Screening in Crystalline Liquids Protects Energetic Carriers in Hybrid Perovskites. *Science* **2016**, *353*, 1409-1413.
20. Munson, K. T.; Doucette, G. S.; Kennehan, E. R.; R., S. J.; Asbury, J. B., Vibrational Probe of the Structural Origins of Slow Recombination in Halide Perovskites. *J. Phys. Chem. C* **2019**, *123*, 7061-7073.
21. Sendner, M.; Nayak, P. K.; Egger, D. A.; Beck, S.; Müller, C.; Epding, B.; Kowalsky, W.; Kronik, L.; Snaith, H. J.; Pucci, A., et al., Optical Phonons in Methylammonium Lead Halide Perovskites and Implications for Charge Transport. *Mater. Horiz.* **2016**, *3*, 613-620.
22. Zhao, D.; Skelton, J. M.; Hu, H.; La-o-vorakiat, C.; Zhu, J.-X.; Marcus, R. A.; Michel-Beyerle, M.-E.; Lam, Y. M.; Walsh, A.; Chia, E. E. M., Low-Frequency Optical Phonon Modes and Carrier Mobility in the Halide Perovskite  $\text{Ch}_3\text{nh}_3\text{pbbr}_3$  Using Terahertz Time-Domain Spectroscopy. *Appl. Phys. Lett.* **2017**, *111*, 201903.

23. Lan, Y.; Dringoli, B. J.; Valverde-Chávez, D. A.; Pонсеа, C. S.; Sutton, M.; He, Y.; Kanatzidis, M. G.; Cooke, D. G., Ultrafast Correlated Charge and Lattice Motion in a Hybrid Metal Halide Perovskite. *Sci. Adv.* **2019**, *5*, eaaw5558.

24. Batignani, G.; Fumero, G.; Srimath Kandada, A. R.; Cerullo, G.; Gandini, M.; Ferrante, C.; Petrozza, A.; Scopigno, T., Probing Femtosecond Lattice Displacement Upon Photo-Carrier Generation in Lead Halide Perovskite. *Nat. Commun.* **2018**, *9*, 1971.

25. Zhu, X. Y.; Podzorov, V., Charge Carriers in Hybrid Organic-Inorganic Lead Halide Perovskites Might Be Protected as Large Polarons. *J. Phys. Chem. Lett.* **2015**, *6*, 4758-4761.

26. Yang, Y.; Ostrowski, D. P.; France, R. M.; Zhu, K.; van de Lagemaat, J.; Luther, J. M.; Beard, M. C., Observation of a Hot-Phonon Bottleneck in Lead-Iodide Perovskites. *Nat. Photon.* **2016**, *10*, 53-59.

27. Hopper, T. R.; Gorodetsky, A.; Frost, J. M.; Müller, C.; Lovrincic, R.; Bakulin, A. A., Ultrafast Intraband Spectroscopy of Hot-Carrier Cooling in Lead-Halide Perovskites. *ACS Energy Lett.* **2018**, *3*, 2199-2205.

28. Niesner, D.; Zhu, H.; Miyata, K.; Joshi, P. P.; Evans, T. J. S.; Kudisch, B. J.; Trinh, M. T.; Marks, M.; Zhu, X. Y., Persistent Energetic Electrons in Methylammonium Lead Iodide Perovskite Thin Films. *J. Am. Chem. Soc.* **2016**, *138*, 15717-15726.

29. Smith, M. D.; Karunadasa, H. I., White-Light Emission from Layered Halide Perovskites. *Acc. Chem. Res.* **2018**, *51*, 619-627.

30. Cortecchia, D.; Yin, J.; Petrozza, A.; Soci, C., White Light Emission in Low-Dimensional Perovskites. *J. Mater. Chem. C* **2019**, *7*, 4956-4969.

31. Lin, H.; Zhou, C.; Tian, Y.; Siegrist, T.; Ma, B., Low-Dimensional Organometal Halide Perovskites. *ACS Energy Lett.* **2018**, *3*, 54-62.

32. McCall, K. M.; Stoumpos, C. C.; Kostina, S. S.; Kanatzidis, M. G.; Wessels, B. W., Strong Electron-Phonon Coupling and Self-Trapped Excitons in the Defect Halide Perovskites  $A_3m_2i_9$  ( $A = Cs, Rb$ ;  $M = Bi, Sb$ ). *Chem. Mater.* **2017**, *29*, 4129-4145.

33. Zelewski, S. J.; Urban, J. M.; Surrente, A.; Maude, D. K.; Schade, L.; Johnson, R. D.; Dollmann, M.; Nayak, P. K.; Snaith, H. J.; Padaelli, P., et al., Revealing the Nature of Photoluminescence Emission in the Metal-Halide Double Perovskite  $Cs_2AgBiBr_6$ . *J. Mater. Chem. C* **2019**, *7*, 8350-8356.

34. Volonakis, G.; Filip, M. R.; Haghaghirad, A. A.; Sakai, N.; Wenger, B.; Snaith, H. J.; Giustino, F., Lead-Free Halide Double Perovskites Via Heterovalent Substitution of Noble Metals. *J. Phys. Chem. Lett.* **2016**, *7*, 1254-1259.

35. Manser, J. S.; Christians, J. A.; Kamat, P. V., Intriguing Optoelectronic Properties of Metal Halide Perovskites. *Chem. Rev.* **2016**, *116*, 12956-13008.

36. Munson, K. T.; Swartzfager, J. R.; Gan, J.; Asbury, J. B., Does Dipolar Motion of Organic Cations Affect Polaron Dynamics and Bimolecular Recombination in Halide Perovskites? *J. Phys. Chem. Lett.* **2020**, *11*, 3166-3172.

37. Nishida, J.; Breen, J. P.; Lindquist, K. P.; Umeyama, D.; Karunadasa, H. I.; Fayer, M. D., Dynamically Disordered Lattice in a Layered Pb-I-Scn Perovskite Thin Film Probed by Two-Dimensional Infrared Spectroscopy. *J. Am. Chem. Soc.* **2018**, *140*, 9882-9890.

38. Park, M.; Neukirch, A. J.; Reyes-Lillo, S. E.; Lai, M.; Ellis, S. R.; Dietze, D.; Neaton, J. B.; Yang, P.; Tretiak, S.; Mathies, R. A., Excited-State Vibrational Dynamics toward the Polaron in Methylammonium Lead Iodide Perovskite. *Nat. Commun.* **2018**, *9*, 2525.

39. Yaffe, O.; Guo, Y.; Tan, L. Z.; Egger, D. A.; Hull, T.; Stoumpos, C. C.; Zheng, F.; Heinz, T. F.; Kronik, L.; Kanatzidis, M. G., et al., Local Polar Fluctuations in Lead Halide Perovskite Crystals. *Phys. Rev. Lett.* **2017**, *118*, 136001.

40. Baikie, T.; Barrow, N. S.; Fang, Y.; Keenan, P. J.; Slater, P. R.; Piltz, R. O.; Gutmann, M.; Mhaisalkar, S. G.; White, T. J., A Combined Single Crystal Neutron/X-Ray Diffraction and Solid-State Nuclear Magnetic

Resonance Study of the Hybrid Perovskites  $\text{Ch}_3\text{nh}_3\text{pb}_x\text{X}_3$  ( $\text{X} = \text{I, Br and Cl}$ ). *J. Mater. Chem. A* **2015**, *3*, 9298-9307.

41. Varadwaj, P. R.; Varadwaj, A.; Marques, H. M.; Yamashita, K., Significance of Hydrogen Bonding and Other Noncovalent Interactions in Determining Octahedral Tilting in the  $\text{Ch}_3\text{nh}_3\text{pb}_3\text{I}_3$  Hybrid Organic-Inorganic Halide Perovskite Solar Cell Semiconductor. *Sci. Rep.* **2019**, *9*, 50.

42. Gallop, N. P.; Selig, O.; Giubertoni, G.; Bakker, H. J.; Rezus, Y. L. A.; Frost, J. M.; Jansen, T. L. C.; Lovrincic, R.; Bakulin, A. A., Rotational Cation Dynamics in Metal Halide Perovskites: Effect on Phonons and Material Properties. *J. Phys. Chem. Lett.* **2018**, *9*, 5987-5997.

43. Bakulin, A. A.; Selig, O.; Bakker, H. J.; Rezus, Y. L. A.; Muller, C.; Glaser, T.; Lovrincic, R.; Sun, Z. H.; Chen, Z. Y.; Walsh, A., et al., Real-Time Observation of Organic Cation Reorientation in Methylammonium Lead Iodide Perovskites. *J. Phys. Chem. Lett.* **2015**, *6*, 3663-3669.

44. Selig, O.; Sadhanala, A.; Müller, C.; Lovrincic, R.; Chen, Z.; Rezus, Y. L. A.; Frost, J. M.; Jansen, T. L. C.; Bakulin, A. A., Organic Cation Rotation and Immobilization in Pure and Mixed Methylammonium Lead-Halide Perovskites. *J. Am. Chem. Soc.* **2017**, *139*, 4068-4074.

45. Taylor, V. C. A.; Tiwari, D.; Duchi, M.; Donaldson, P. M.; Clark, I. P.; Fermin, D. J.; Oliver, T. A. A., Investigating the Role of the Organic Cation in Formamidinium Lead Iodide Perovskite Using Ultrafast Spectroscopy. *J. Phys. Chem. Lett.* **2018**, *9*, 895-901.

46. Ghosh, D.; Walsh Atkins, P.; Islam, M. S.; Walker, A. B.; Eames, C., Good Vibrations: Locking of Octahedral Tilting in Mixed-Cation Iodide Perovskites for Solar Cells. *ACS Energy Lett.* **2017**, *2*, 2424-2429.

47. Herz, L. M., How Lattice Dynamics Moderate the Electronic Properties of Metal-Halide Perovskites. *J. Phys. Chem. Lett.* **2018**, *9*, 6853-6863.

48. Katan, C.; Mohite, A. D.; Even, J., Entropy in Halide Perovskites. *Nat. Mater.* **2018**, *17*, 377-379.

49. Wright, A. D.; Verdi, C.; Milot, R. L.; Eperon, G. E.; Pérez-Osorio, M. A.; Snaith, H. J.; Giustino, F.; Johnston, M. B.; Herz, L. M., Electron-Phonon Coupling in Hybrid Lead Halide Perovskites. *Nat. Commun.* **2016**, *7*, 11755.

50. Seiler, H.; Palato, S.; Sonnichsen, C.; Baker, H.; Socie, E.; Strandell, D. P.; Kambhampati, P., Two-Dimensional Electronic Spectroscopy Reveals Liquid-Like Lineshape Dynamics in  $\text{CsPbI}_3$  Perovskite Nanocrystals. *Nat. Commun.* **2019**, *10*, 4962.

51. Cinquanta, E.; Meggiolaro, D.; Motti, S. G.; Gandini, M.; Alcocer, M. J. P.; Akkerman, Q. A.; Vozzi, C.; Manna, L.; De Angelis, F.; Petrozza, A., et al., Ultrafast Thz Probe of Photoinduced Polarons in Lead-Halide Perovskites. *Phys. Rev. Lett.* **2019**, *122*, 166601.

52. Tan, H.; Che, F.; Wei, M.; Zhao, Y.; Saidaminov, M. I.; Todorović, P.; Broberg, D.; Walters, G.; Tan, F.; Zhuang, T., et al., Dipolar Cations Confer Defect Tolerance in Wide-Bandgap Metal Halide Perovskites. *Nat. Commun.* **2018**, *9*, 3100.

53. Lewis, D. J., Chapter 10 Deposition Techniques for Perovskite Solar Cells. In *Nanostructured Materials for Type III Photovoltaics*, The Royal Society of Chemistry: 2018; pp 341-366.

54. Herz, L. M., Charge-Carrier Dynamics in Organic-Inorganic Metal Halide Perovskites. *Ann. Rev. Phys. Chem.* **2016**, *67*, 65-89.

55. Munson, K. T.; Grieco, C.; Kennehan, E. R.; Stewart, R. J.; Asbury, J. B., Time-Resolved Infrared Spectroscopy Directly Probes Free and Trapped Carriers in Organo-Halide Perovskites. *ACS Energy Lett.* **2017**, *2*, 651-658.

56. Munson, K. T.; Kennehan, E. R.; Asbury, J. B., Structural Origins of the Electronic Properties of Materials Via Time-Resolved Infrared Spectroscopy. *J. Mater. Chem. C* **2019**, *7*, 5889-5909.

57. Kiermasch, D.; Rieder, P.; Tvingstedt, K.; Baumann, A.; Dyakonov, V., Improved Charge Carrier Lifetime in Planar Perovskite Solar Cells by Bromine Doping. *Sci. Rep.* **2016**, *6*, 39333.

58. Emin, D., Optical-Properties of Large and Small Polarons and Bipolarons. *Phys. Rev. B* **1993**, *48*, 13691-13702.

59. Xing, G.; Wu, B.; Wu, X.; Li, M.; Du, B.; Wei, Q.; Guo, J.; Yeow, E. K. L.; Sum, T. C.; Huang, W., Transcending the Slow Bimolecular Recombination in Lead-Halide Perovskites for Electroluminescence. *Nat. Commun.* **2017**, *8*, 14558.

60. Era, M.; Morimoto, S.; Tsutsui, T.; Saito, S., Organic-Inorganic Heterostructure Electroluminescent Device Using a Layered Perovskite Semiconductor (C<sub>6</sub>h5c2h4nh<sub>3</sub>)<sub>2</sub>pbi4. *Appl. Phys. Lett.* **1994**, *65*, 676-678.

61. Hong, X.; Ishihara, T.; Nurmikko, A. V., Photoconductivity and Electroluminescence in Lead Iodide Based Natural Quantum Well Structures. *Solid State Commun.* **1992**, *84*, 657-661.

62. Wong, W. P. D.; Yin, J.; Chaudhary, B.; Chin, X. Y.; Cortecchia, D.; Lo, S.-Z. A.; Grimsdale, A. C.; Mohammad, O. F.; Lanzani, G.; Soci, C., Large Polaron Self-Trapped States in Three-Dimensional Metal-Halide Perovskites. *ACS Materials Lett.* **2020**, *2*, 20-27.

63. Chen, T.; Chen, W.-L.; Foley, B. J.; Lee, J.; Ruff, J. P. C.; Ko, J. Y. P.; Brown, C. M.; Harriger, L. W.; Zhang, D.; Park, C., et al., Origin of Long Lifetime of Band-Edge Charge Carriers in Organic-Inorganic Lead Iodide Perovskites. *Proc. Nat. Acad. Sci.* **2017**, *114*, 7519-7524.

64. Kubicki, D. J.; Prochowicz, D.; Hofstetter, A.; Péchy, P.; Zakeeruddin, S. M.; Grätzel, M.; Emsley, L., Cation Dynamics in Mixed-Cation (Ma)X(Fa)1-Xpbi3 Hybrid Perovskites from Solid-State Nmr. *J. Am. Chem. Soc.* **2017**, *139*, 10055-10061.

65. Ambrosio, F.; Meggiolaro, D.; Mosconi, E.; De Angelis, F., Charge Localization, Stabilization, and Hopping in Lead Halide Perovskites: Competition between Polaron Stabilization and Cation Disorder. *ACS Energy Lett.* **2019**, *4*, 2013-2020.

66. Yang, B.; Ming, W.; Du, M.-H.; Keum, J. K.; Puretzky, A. A.; Rouleau, C. M.; Huang, J.; Geohegan, D. B.; Wang, X.; Xiao, K., Real-Time Observation of Order-Disorder Transformation of Organic Cations Induced Phase Transition and Anomalous Photoluminescence in Hybrid Perovskites. *Adv. Mater.* **2018**, *30*, 1705801.

67. Chen, Y.; Yi, H. T.; Wu, X.; Haroldson, R.; Gartstein, Y. N.; Rodionov, Y. I.; Tikhonov, K. S.; Zakhidov, A.; Zhu, X. Y.; Podzorov, V., Extended Carrier Lifetimes and Diffusion in Hybrid Perovskites Revealed by Hall Effect and Photoconductivity Measurements. *Nat. Commun.* **2016**, *7*, 12253.

68. Neukirch, A. J.; Nie, W.; Blancon, J.-C.; Appavoo, K.; Tsai, H.; Sfeir, M. Y.; Katan, C.; Pedesseau, L.; Even, J.; Crochet, J. J., et al., Polaron Stabilization by Cooperative Lattice Distortion and Cation Rotations in Hybrid Perovskite Materials. *Nano Lett.* **2016**, *16*, 3809-3816.

69. Dastidar, S.; Li, S.; Smolin, S. Y.; Baxter, J. B.; Fafarman, A. T., Slow Electron–Hole Recombination in Lead Iodide Perovskites Does Not Require a Molecular Dipole. *ACS Energy Lett.* **2017**, *2*, 2239-2244.

70. Schlipf, M.; Poncé, S.; Giustino, F., Carrier Lifetimes and Polaronic Mass Enhancement in the Hybrid Halide Perovskite \${\rm \mathcal{M}(\mathcal{C}h)}\_3{\rm \mathcal{N}h}\_3{\rm \mathcal{P}bi}\_3\$ from Multiphonon Fr\"Ohlich Coupling. *Phys. Rev. Lett.* **2018**, *121*, 086402.

71. Bischak, C. G.; Wong, A. B.; Lin, E.; Limmer, D. T.; Yang, P.; Ginsberg, N. S., Tunable Polaron Distortions Control the Extent of Halide Demixing in Lead Halide Perovskites. *J. Phys. Chem. Lett.* **2018**, *9*, 3998-4005.

72. Fisicaro, G.; La Magna, A.; Alberti, A.; Smecca, E.; Mannino, G.; Deretzis, I., Local Order and Rotational Dynamics in Mixed a-Cation Lead Iodide Perovskites. *J. Chem. Phys. Lett.* **2020**, *11*, 1068-1074.

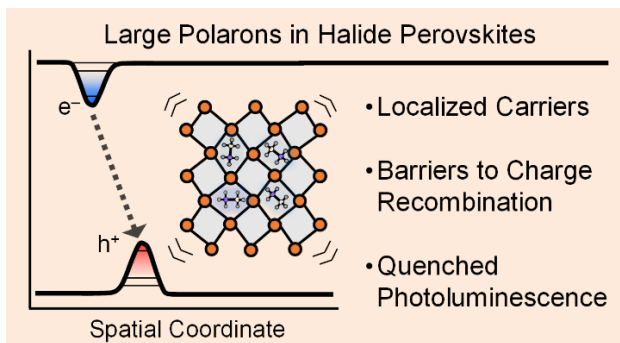
73. Tan, H.; Che, F.; Wei, M.; Zhao, Y.; Saidaminov, M. I.; Todorovic, P.; Broberg, D.; Walters, G.; Tan, F.; Zhuang, T., et al., Dipolar Cations Confer Defect Tolerance in Wide-Bandgap Metal Halide Perovskites. *Nat. Commun.* **2018**, *9*, 3100.

74. Dagnall, K. A.; Foley, B. J.; Cuthriell, S. A.; Alpert, M. R.; Deng, X.; Chen, A. Z.; Sun, Z.; Gupta, M. C.; Xiao, K.; Lee, S.-H., et al., Relationship between the Nature of Monovalent Cations and Charge Recombination in Metal Halide Perovskites. *ACS Appl. Energy Mater.* **2020**, *3*, 1298-1304.

75. Nishida, J.; Alfaifi, A. H.; Gray, T. P.; Shaheen, S. E.; Raschke, M. B., Heterogeneous Cation–Lattice Interaction and Dynamics in Triple-Cation Perovskites Revealed by Infrared Vibrational Nanoscopy. *ACS Energy Lett.* **2020**, *5*, 1636-1643.

76. Adriaenssens, G. J.; Arkhipov, V. I., Non-Langevin Recombination in Disordered Materials with Random Potential Distributions. *Solid State Commun.* **1997**, *103*, 541-543.

## TOC Graphic



## Author Biographies



**Kyle T. Munson** earned a bachelor's degree in chemistry from Rowan University in Glassboro, NJ in 2015. While at Rowan, he studied proton solvation and conduction mechanisms in ionic liquids. He was an NSF Graduate Research Fellow in the Department of Chemistry at the Pennsylvania State University working with Professor John Asbury examining the structural origins of the electronic properties of halide perovskites using mid-IR transient absorption spectroscopy. Currently, he is at the Materials Research Institute at the Pennsylvania State University developing an ultrafast transient absorption microscope to examine the electronic properties of 2-Dimensional materials with controlled doping characteristics.



**John B. Asbury** is a professor of chemistry at the Pennsylvania State University and co-founder of Magnitude Instruments. His research program focuses on development of ultrafast spectroscopy and microscopy techniques to understand how the electronic properties of materials evolve from their molecular and crystalline structure. Before coming to Penn State in 2005, Asbury completed his Ph.D. in chemistry at Emory University working with Tianquan (Tim) Lian to investigate interfacial electron transfer dynamics in dye sensitized metal oxides. His post-doctoral work at Stanford University with Michael Fayer focused on development of 2D IR spectroscopy of hydrogen bond dynamics in water.